Dynamic analysis of a steel footbridge under running pedestrians

M.G. Mulas & M. Pisani
Department of Civil and Environmental Engineering, DICA; Politecnico di Milano, Milano, Italy

F. Beeckmans
Mc-Carré SPRL, Louvain-la-Neuve, Belgium

P. Latteur
Université Catholique de Louvain, Louvain-la-Neuve, Belgium

ABSTRACT: The paper presents the studies on the serviceability conditions of a footbridge to be built in Louvain-La-Neuve (Belgium). The preliminary design was performed by the Engineering Company Mc Carré. The 5-span steel footbridge is 54 m long. The central span is supported by two inclined arches. First, the modelling approach for the structure, aimed to determine its modal properties and to spot possible resonant problem under moving pedestrians, is discussed. The finite element model, developed within the ANSYS framework, does not possess any natural frequency in the critical range excited by walking pedestrians but one frequency is in the range excited by running pedestrians. To investigate the bridge response to a running pedestrian, different approaches of analysis are adopted. Harmonic analysis follows indications from HiVoSS 2008. Three models of moving load are adopted in transient analysis, the two load models in Setra 2006 and the model by Racic & Morin 2014. Results highlight the importance of proper consideration to the effect of running pedestrians, and the need for more accurate guidelines.

1 INTRODUCTION

Human induced loads brought to structural collapses rarely, but are very important for serviceability conditions. In the last years, the adoption of light materials pushed towards the design of light and slender footbridges, whose natural frequencies fall often in the interval that characterizes loads induced by walking, running or jumping pedestrians. The well-known case of Millennium Bridge in London (Dallard et al. 2001) generated a large research effort of the scientific and engineering community on the problem of predicting or avoiding excessive vibrations. Several mathematical models of the human induced loads (ground reaction forces, GRFs), based on biomechanics, were proposed for the application in the civil engineering field. Deterministic, stochastic and mechanical models aim also to reproduce inter- and intra-subjects' variability, linked to several variables such as stiffness of the walking surface, the speed of movement or the crowd density (Živanović 2015). Since the perception of vibrations was found to be dependent on the same variables, acceleration is considered as the control parameter at the design phase to assess the serviceability limit state of a footbridge (Živanović et al 2005).

However, little attention has been paid up to now to the problem of running pedestrians, even though critical vibration could arise both in case of a crowd of running pedestrians, as in a marathon, or due to runners crossing the bridge while other pedestrians are walking. Lai et al 2017 detected, on a lively footbridge, a value of acceleration due to four running pedestrians almost four times higher than that due to four walking pedestrians.

Aim of this paper is to perform a numerical assessment of a footbridge to running pedestrians, to evaluate both the relevance of the load induced by runners and the models available in the literature. The case study is a steel footbridge to be built in Louvain-La-Neuve (Belgium). To investigate the dynamic properties of the footbridge, three finite elements (FE) models of the bridge are derived with Ansys Mechanical APDL. One model has the geometry defined in design and two have modifications in the arches geometry. The design configuration has a natural frequency in the critical range for running pedestrians. Dynamic analyses, either harmonic or transient, are performed. The former follows the HiVoSS 2008. The latter adopts three load models, two from Setra 2006 and one, based on experimental data, proposed by Racic & Morin 2014. To account for the spatial and temporal variability of the load, an innovative approach is adopted in transient analyses, to apply the load time histories, computed with the three load models, to the footbridge FE model.

In the following, Section 2 describes the geometry and the FE model of the footbridge. Section 3 discusses the pedestrian modeling. Results of numerical analyses are presented in Section 4. A few conclusions are drawn in Section 5.

2 THE FOOTBRIDGE

2.1 *Geometry description*

The preliminary design of the steel footbridge at study (Fig. 1), to be built in Louvain La Neuve (Belgium), was carried out by the Engineering office Mc Carré according to Eurocode EN1993. Design loads follow prescriptions of EC1991-2:2003 and Hivoss guidelines. In static conditions a pedestrian load of 500kg/m^2 is considered. Two-axle (spaced apart 3m) service vehicles, 35 kN heavy, can cross the bridge.

Two plane arches support the central part of the deck. Each of them represents an arch of a circumference with radius of 27 m and subtended angle of 75°. The arch planes are inclined of 15° with respect to the vertical plane, being nearer each other at their bases (Fig. 2). Arches cross-sections are L-shaped and their dimensions vary linearly from the supports, where the cross-section depth is larger than its width (500×200×20 mm), to the top, where the contrary holds true (300×550×20 mm).

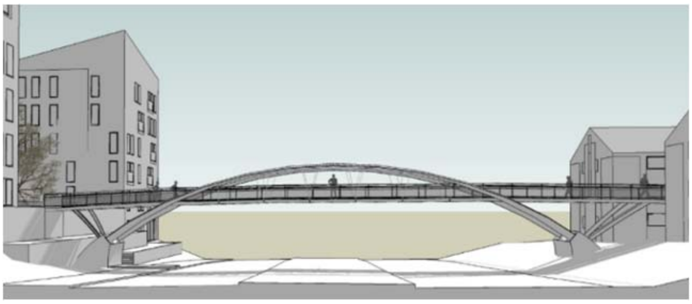

Figure 1. Lateral view of the structure: the footbridge links the Lauzelle District (left) with the Courbevoie District (right).

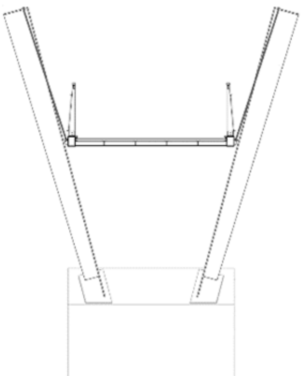

Figure 2. Section of the footbridge at the central span.

The footbridge is symmetric with respect to the longitudinal axis. The 54 m long deck is subdivided in 5 spans by intersection points with arches and struts elements. The central span of the structure is linked to each arch trough ten suspension cables (ϕ=25 mm). The structure of the deck is a grid (Fig. 3b). The main longitudinal beams, 54 m long, are placed on the edges of the deck, spaced 3.15 m apart. Their cross-section is a hollow rectangle 200×150×10 mm. Transversal elements, with the standard European rolled-steel HEB100 shape, are placed every 1.60 m. Secondary longitudinal T-shaped elements (100×100×9 mm), spaced 0.60 m apart, connect the HEB100 beams longitudinally. Connections among steel elements are all welded. Cables (ϕ=20 mm) ensure bracing in the horizontal plane of the grid structure. The steel grid is covered by a wood plank. The two sides of arches are linked to the ground through concrete footings. Four struts elements with a double inclination (Fig. 3a) link the deck to the ground through the same concrete footings. Struts have a H-tapered cross-section.

Steel S235 and S460N are used for arches, struts and deck grid and for suspension cables, respectively. Wood density is 1050 kg/m^3.

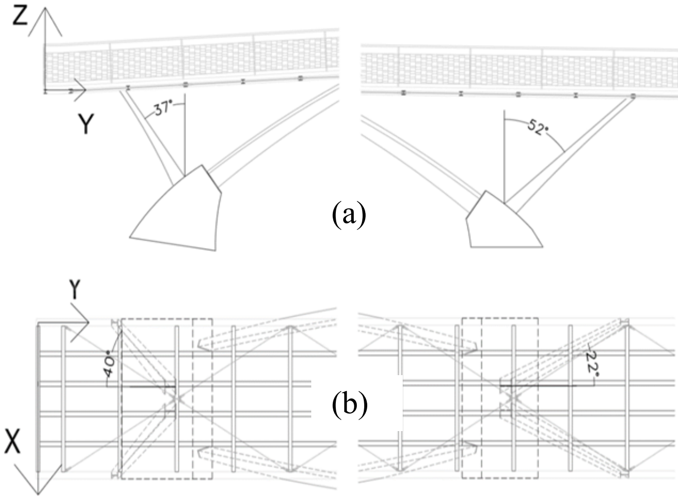

Figure 3 Details of struts inclinations: (a) lateral view; (b) in-plane view.

2.2 *FE model*

The FE model of the footbridge was developed with a student license of Ansys Mechanical APDL. To explore different bridge configurations two additional cases were considered (Fig. 4).

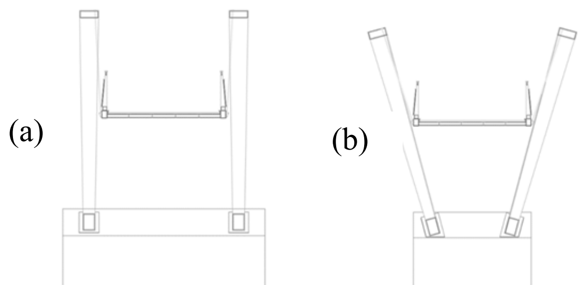

Figure 4. Sections at central span of models: a) A, b) B.

In the simpler Model A, vertical arches have a hollow rectangular cross-section, retaining the variability of dimensions along the arch. In a second intermediate model, named B, the correct arches inclination was inserted. The as-designed geometry is considered in Model C (Fig. 2).

In the FE models, the girders of both the steel grid and the arches are modeled with a Timoshenko beam element named “BEAM 188”, with 6 degrees of freedom (DOFs) at each node. Cables and braces are modeled with "LINK 180", a spar element transmitting axial force only, with 3 DOFs at each node. Timber planks and handrails are modeled as lumped masses on steel grid; their weight is included in the dead load. The boundary conditions of the footbridge model, as the constraint conditions between adjacent elements, are inferred from the technical drawings. Cable pretension, not foreseen in the preliminary design, is applied to cables. With a trial and error procedure, pretension values were determined to compensate the sag due to dead load. A preliminary non-linear static analysis accounts for the cables geometric stiffness and the variation of configuration associated to dead loads. The FE model C is depicted in Figure 5.

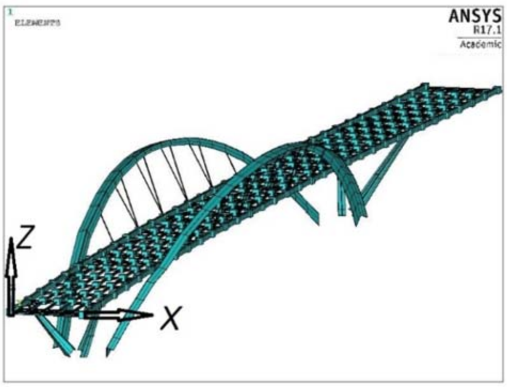

Figure 5. FE model of the as-designed footbridge at study.

The first 10 natural frequencies, computed considering masses from dead load only, are listed in Table 1 for the three models. The "Mode type" column describes the predominant deformation of each mode shape: "A" refers to arches deformation; "+D" is added if a significant deformation of the deck is observed. The abbreviations "L", "V" and "T" denote a lateral, vertical or torsional natural mode.

n°	f_A [Hz]	Mode type	f_B [Hz]	Mode type	f_C [Hz]	Mode type
1	2.03	A (L)	2.01	A(L)	1.12	A (L)
2	3.59	A (L) + D (V)	3.52	(V)	1.56	A (L)
3	3.63	(V)	3.53	(V)	2.74	A (L)
4	3.96	(L)	3.62	(L)	3.38	(L) +(T)
5	4.51	(T)	4.53	(T)	3.60	(V)
6	5.51	(L)	5.38	(T)	4.27	A (L)
7	6.92	(V)	6.90	(V)	4.78	(L) +(T)
8	6.94	(T)	6.91	(T)	6.19	(V)
9	7.13	(V)	7.03	(V)	6.29	(T)
10	7.28	(V)+(T)	7.06	(T)	6.42	(V)

Table 1 Eigenfrequencies of the three FE models

Table 1 shows that the structural geometry significantly affects the frequency values. Lateral, vertical, torsional and mixed modes of vibrations appear, having different frequencies. Although variations of frequencies values may be not significant, for a given mode, deformed shapes can be very different among the three models. In particular, the adoption of an open cross-section for arches makes the structure more prone to arches vibrations.

Figure 6 compares the frequencies listed in Table 1. Values for models A and B are very close; those of Model C are always smaller. It can be concluded that the predominant effect producing the stiffness increase of Model A is the closed cross-section rather than the verticality of arches.

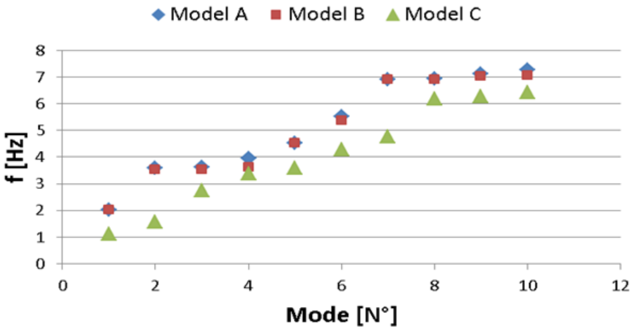

Figure 6. Natural frequencies of the three models.

3 PEDESTRIAN MODELING

3.1 *Pedestrian movement: running*

The walking pedestrian induced load, named Ground Reaction Force (GRF), has three components: vertical, longitudinal and lateral. Figure 7 depicts the typical M-shaped vertical component. Steps come in a sequence during a walk; in each step there are two time intervals in which only a foot is in contact with the ground (single support phase, SSP) and an intermediate time in which both feet touch the ground (double support phase, DSP). Studies on the relation between the pedestrian's velocity and the duration of SSP and DSP showed that, as speed increases, the duration of DSP decreases and vanishes when the pedestrian starts to run. Moreover, also the time history load shape was found to be dependent on the speed (Keller et al. 1996). In the running gait cycle the so-called flying phase (FP) appears, when no foot is on the ground and the load shape has a single peak (see Fig. 8).

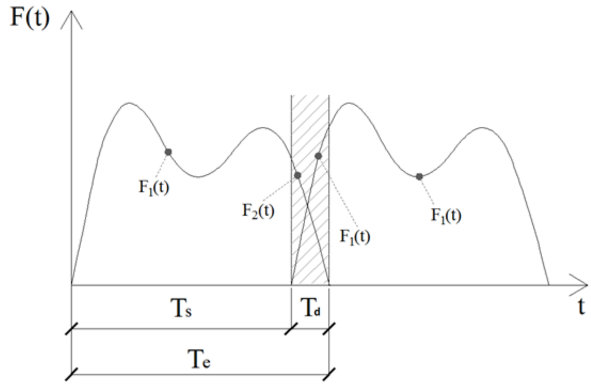

Figure 7. Time history of GRF vertical component for a walking pedestrian for a complete step (Mulas et al 2018).

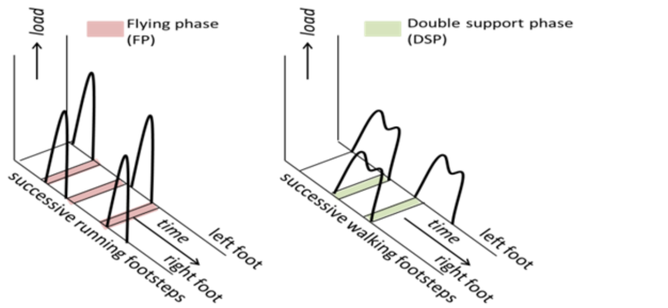

Figure 8. 3D Vertical components of GRFs, running and walking, for both feet and two different velocities.

3.2 *Running force models*

The Hivoss guideline for running pedestrians prescribes a serviceability check when the step frequency f_s is $1.9<f_s<3.5$Hz. The proposed model is a single load $P(t,v)$ moving across the bridge with the velocity v of the jogger:

$$P(t,v) = P\cos(2\pi f_s t) \times n'\psi \tag{1}$$

In (1), f_s is the step frequency, P is the force component due to a single pedestrian moving with step frequency f_s, n' is the equivalent number of pedestrians on the loaded surface S. The reduction coefficient ψ, taking into account the probability that the footfall frequency approaches the natural frequency under consideration, varies linearly from 0 to 1 between 1.9 and 2.2 Hz and from 1 to 0 between 2.7 and 3.5 Hz, while is equal to 1 in the range 2.2-2.7 Hz and zero elsewhere. Alternatively, the guideline suggests to load the point where the mode shape has the maximum displacement amplitude with a force $P(t,v=0)$.

The SETRA guideline proposes two load models. One reproduces the force generated by the runner with the positive values of a sine function (Fig. 9a). Thus, the vertical component $F(t)$ of the GRF is:

$$F(t) = k_P G_0 \sin\left(\frac{\pi t}{t_P}\right) \qquad (j-1)T_m \le t \le (j-1)T_m + t_p \tag{2}$$

$$F(t) = 0 \qquad (j-1)T_m + t_p \le t \le jT_m = 0 \tag{3}$$

In (2) and (3) k_P is the impact factor ($k_P = \frac{F_{max}}{G_0}$); j is the step number; F_{max} is the maximum load; $G_0$is the pedestrian weight; t_P is the contact duration and T_m is given by $1/f_m$, f_m being the frequency of running. The second SETRA model retains the null value for $F(t)$ in the interval in (3), while adopting a Fourier series of three sine functions (Fig. 9b), whose parameters G_i are given as a function of step frequency and velocity, in the same time interval of (2):

$$F(t) = G_0 + \sum_{i=1}^{n} G_i \sin(2\pi i f_m t) \tag{4}$$

In the analyses, T_m=0.295s and t_P=0,5T_m is assumed.

The model of Racic & Morin (2014) (R&M) here adopted is based on an experimental campaign, providing 458 individual running force signals, recorded by two state-of-the-art instrumented treadmills. The model accounts for both intra- and inter-variability of the running forces. Their quasi-periodic nature gives raise to a narrow band stochastic process. The model is a *generator* of random near-periodic signals, based on the definition of a *template cycle* extracted from experimental data at a selected frequency. The curve fit $Z(t)$ of the template cycle is the sum of four Gaussian functions:

$$Z(t) = \sum_{i=1}^{4} A_i e^{-(t-t_i)^2/2\delta_i^2} \tag{5}$$

In (5), A_i is the height of the jth Gaussian peak; t_i is the position of the center of the peak; δ_i controls the width of the Gaussian bell functions. The variability of cycles duration and of force amplitude is accounted for too (reader is referred to the original work for details).

Figure 9 compares a few load cycles for each of the three models. Pedestrian weight is 605 N, step frequency f_s is 3.38 Hz. The different frequency content of the three signals is readily appreciated.

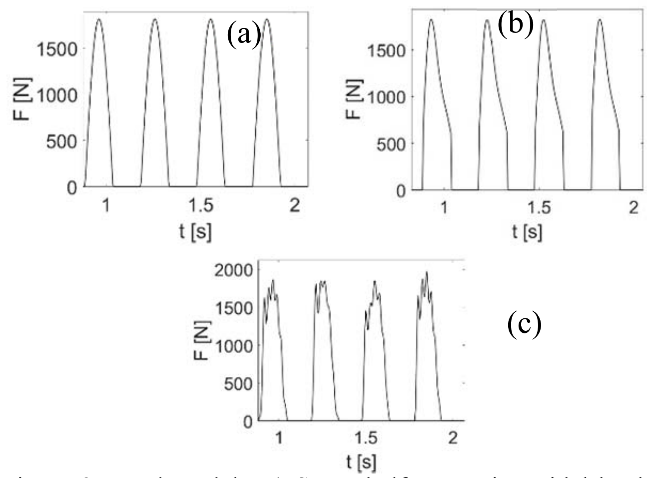

Figure 9. Load models: a) Setra, half-wave sinusoidal load; b) Setra, Fourier load; c) Racic & Morin 2014 model.

3.3 *Transient analysis under moving loads*

The load time-histories generated by a running pedestrian, shown at Section 3.2, are implicitly associated to a variation of the force in space. Load cycles are identified by a contact phase and a flying phase, and the distance between two consecutive contact points is the pedestrian stride length. Given the pedestrian motion, it is possible to identify the position of the contact points on the bridge. However, in general these will not coincide with the nodes of the mesh grid. A set of proper shape functions is adopted to transform contact forces into nodal loads, following the approach of Mulas et al 2018 (Fig. 10). An ad-hoc Matlab script named RealRun1 handles the transformation of contact forces into nodal loads, providing the input data for Ansys APDL.

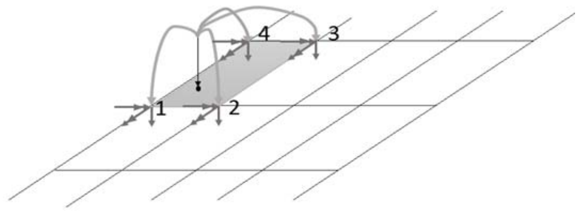

Figure 10. Shape functions transform a vertical force into nodal forces and bending moments.

4 NUMERICAL ANALYSES

The FE (as-designed) model C was numerically analysed. A Rayleigh damping was adopted, with a damping ratio equal to 0.4 (HiVoss 2008) for the first two modes. In harmonic analysis, the load (1) is applied to node 79 (see Fig. 11), the one having the largest displacement amplitude in the 4^{th} mode shape (f_4= 3.38 Hz). In transient analyses, the first contact point has coordinates x=0.2m, y=0.1m and z=0 in the global reference system of Figure 5. Since the pedestrian's trajectory is rectilinear, x remains constant during the whole time history. The runner velocity is 6.6m/s, with a crossing time of 8.17 s. Results are analyzed at three nodes in each span but the first (a very short one), as showed in Figure 12.

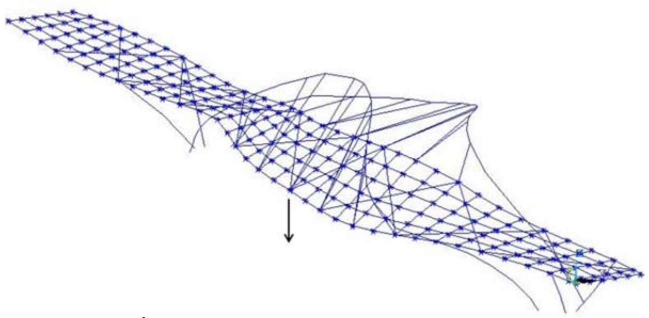

Figure 11. 4^{th} mode shape; an arrow denotes the harmonic load at node 79.

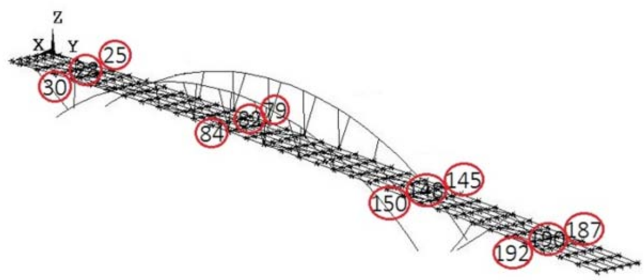

Figure 12. Nodes where results are analyzed.

Figure 13 shows the results of the harmonic analysis, in terms of acceleration amplitude. The largest values are found in the middle span, at nodes 79 and 84. A torsional effect is apparent in the same span. At node 79, the amplitude of vertical displacement and acceleration is equal to 1.3 mm and to 0.562 m/s^2, respectively. According to the HiVoss guideline, the latter is above the threshold for Comfort Class 1 (0.5 m/s^2) but still guarantees a medium degree of comfort (a_{max}< 1m/s^2).

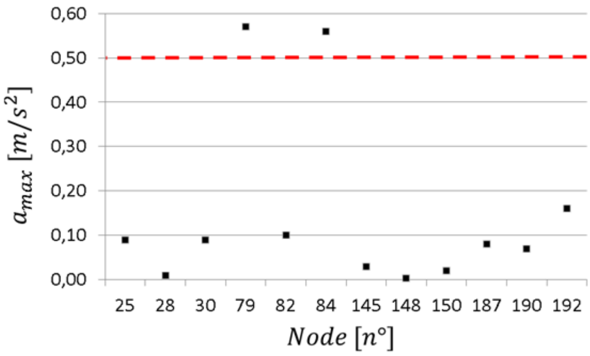

Figure 13. Harmonic analysis, acceleration peak at selected nodes. The dashed line is the threshold for Comfort Class 1.

In transient analyses, the pedestrian enters the bridge from the left (Fig. 12), following a rectilinear trajectory along the left edge, from node 25 towards node 187. The frequency of contact between runner and structure is 3.38Hz, as in the harmonic analysis. In the R&M model, T_m varies between 0.26 and 0.335s; t_P varies accordingly. The step length is 1.99 m. The extreme absolute values of acceleration, at nodes on the footbridge edges and for each of the load models, are shown in Table 2.

Node	a_{max} R&M $[m/s^2]$	a_{max} Sin $[m/s^2]$	a_{max} Four $[m/s^2]$
25	1.80	0.62	2.26
30	1.38	0.39	1.84
79	1.05	0.88	0.88
84	1.01	1.00	1.08
145	3.99	3.71	3.47
150	3.88	3.72	3.78
187	7.37	5.68	5.04
192	7.3	7.37	6.07

Table 2. Transient analyses, acceleration peak values. First column, R&M model; second column, half-wave sinus model; third column, Fourier series.

For all the models, in each cross-section the values of acceleration are higher in the nodes loaded directly by the pedestrian. For the last two nodes (187 and 192), the opposite holds true, coherently with the shape of the excited torsional mode. The same pattern is found also in Figure 13. Extreme values increase as the time necessary to the pedestrian to reach the node. Discrepancies among the three models are larger at the bridge entrance, where the scatter among the results is quite high, tend to disappear in the central part and increase again at the bridge end. Starting from node 79, the results of the half-wave sinus model are intermediate between those of the R&M and Fourier models. Moreover, the Fourier model overestimates acceleration of limited value (eg at node 25) and underestimates large values, as it is found at nodes of the second (25-30) and fifth span (187-192). A good agreement in the pattern of the results for the three models is detected.

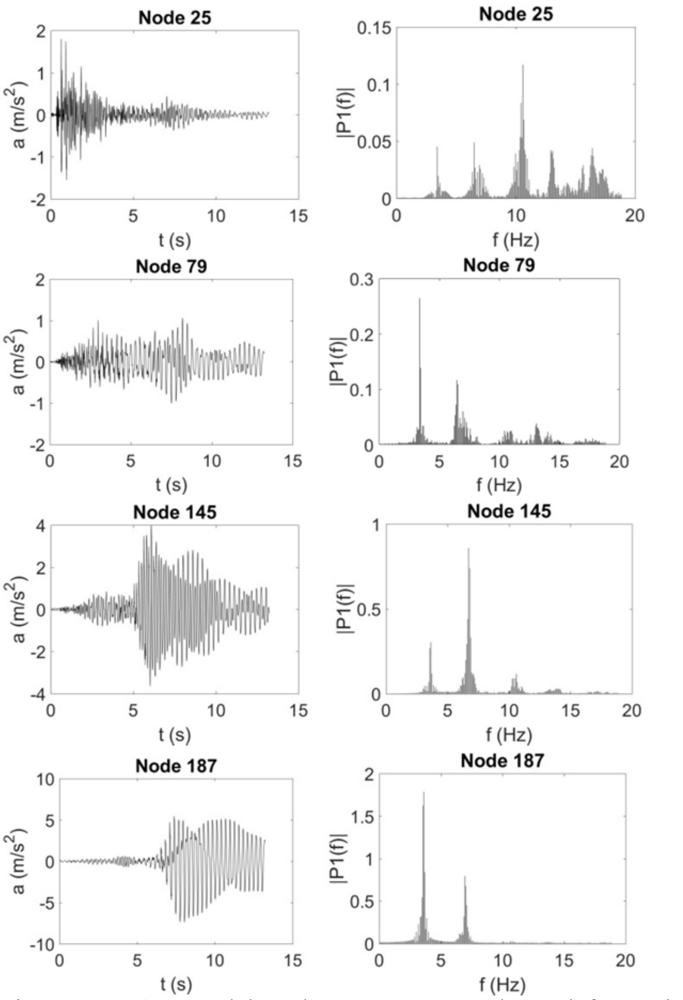

Figure 14. R&M model, nodes 25, 79, 145 and 187: left, accelerations, right, single sided amplitude spectra.

Figure 14 shows the acceleration time histories and the amplitude of the related single sided spectra, for the nodes along the runner's trajectory. The results clarify the outcome of Table 2: a resonant phenomenon is apparent in the final part of the bridge, with accelerations increasing as the elapsed time. The nodes at the two bridge ends are excited mainly when are loaded directly, while the central part of the bridge (e.g. node 79) vibrates with the same intensity during the whole time history. Accelerations exceed significantly the comfort limits. Peak values at node 145, 150 and 186 are of the same order of magnitude of those experimentally recorded at the Seriate footbridge (Lai et al, 2017). Spectra show significant components not only on the first load harmonic, but also on the second (7.76Hz)

A large discrepancy is found between the results of the harmonic and the transient analysis. For the nodes along the trajectory of the runner (25-79-145-187), the mean value of the vertical acceleration was around 0.15 m/s^2 with a peak of 0.57 m/s^2 according to HiVoss and around 3.01 m/s^2 with a peak of 5.95 m/s^2 using RealRun1. In particular, node 79, the most excited by HiVoss prescription, has a maximum acceleration equal to 1.05 m/s^2 according to R&M, much smaller than those recorded at nodes in the 4th and 5th span, but almost double of the value predicted by HiVoss.

5 CONCLUSIONS

This works presents the numerical serviceability assessment of a footbridge, still at the design phase, having a frequency in the critical range for running. Different analysis and modeling approaches are adopted. Harmonic analysis (HiVoss 2008) at the critical frequency underestimates by almost an order of magnitude the acceleration determined with transient analyses. The harmonic load is applied to the node with the largest amplitude for the considered mode shape, but transient analyses detect extreme acceleration values at node 187, with the largest static displacement. Transient analyses exploits three load models (from Setra 2006 and R&M 2014), varying in time and space to simulate the runner's motion. The pattern of variation of peak acceleration along the bridge is similar for the most accurate R&M model and the SETRA models, but values are close only in the central part of the bridge. Time histories in different nodes show the presence of a resonant phenomenon. Acceleration exceed values experimentally recorded. Results for the case study indicate the need for serviceability assessment for runners induced loads. The footbridge design was modified after the completion of this study.

6 REFERENCES

ANSYS. 2015. Online Manuals Release 5.5, <http://mostreal.sk/html/guide_55/GBooktoc.html>.

Eurocode EC1991-2:2003. 2003. Eurocode 1: Actions on structures - Part 2: Traffic loads on bridges.

Dallard, P., Fitzpatrick, T., Flint, A., Low, A., Ridsdill-Smith, R., Willford, M., Roche, M. 2001. London Millennium Bridge: pedestrian-induced lateral vibration, *J. of Bridge Engineering* 6 (6): 412-417.

Keller, T.S, Weisberger, A.M, Ray, J.L, Hasan, S.S, Shiavi, R.G, Spengler, D.M. 1996. Relationship between vertical ground reaction force and speed during walking, slow jogging and running. *Clinical Biomechanics* 11: 253-259.

Lai E., Gentile C., Mulas M.G. 2017. "Experimental and numerical serviceability assessment of a steel suspension footbridge", *J. of Construct. Steel Research*, 132: 16-28.

Mulas M.G., Lai, E. & Lastrico, G. 2018. Coupled Analysis of Footbridge-Pedestrian Dynamic Interaction, *Engineering Structures*, 176: 127-142.

Racic, V. & Morin, J.B. 2014. Data-driven modelling of vertical dynamic excitation of bridges induced by people running. Mech. Systems and Signal Processing 43: 153-170.

Racic, V., Pavic, A. & Brownjohn, J.M.W. 2009. Experimental identification and analytical modelling of human walking forces: Literature review. *J. Sound and Vibration* 326: 1-49.

Research Fund for Coal and Steel. 2008. *HiVoSS*: Design of footbridges. Background Document.

Sétra. 2006. Evaluation du comportement vibratoire des passerelles piétonnes sous l'action des piétons.

Živanović, S. 2015. Modelling human actions on lightweight structures: experimental and numerical developments. *MATEC Web of Conferences*, 24: 01005.

Živanović, S., Pavic, A., Reynolds, P. 2005. Vibration serviceability of footbridges under human-induced excitation: a literature review, *J. of Sound and Vibration* 279: 1-74